ISBN: 978-3-95450-132-8 doi:10.18429/JACoW-IPAC2014-TUPME031

RADIATION PRESSURE ACCELERATION AND TRANSPORT METHODS*

P. Schmidt†, O. Boine-Frankenheim‡, TU-Darmstadt, Darmstadt, Germany
I. Hofmann§, GSI, Darmstadt, Germany

Abstract

Laser acceleration [3, 4] has become an interesting field of research in the past years. Several experiments, such as LIGHT [1, 2] are performed worldwide. High intense, pulsed laser beams are used to generate and accelerate a plasma. The most recent acceleration mechanism is the Target Normal Sheath Acceleration (TNSA) [5]. Light ions (e.g. protons) on the surface of the target are accelerated to energies in the range of 3MeV-50MeV with an exponentially distribution. Going to higher laser intensities ($> 10^{21}$ Wcm^{-1}), a new acceleration mechanism occurs: the Radiation Pressure Acceleration (RPA). The entire foil target is accelerated by the radiation pressure of the laser pulse [6, 7]. Ideally, a sharp peak spectrum is generated with energies up to GeV and nearly solid body density. This work faces on a detailed analysis of the acceleration mechanism in order to develop strategies to efficiently transport the generated beam. 1D and 2D simulations (PIC and fluid) are used to obtain the phase-space distribution of the beam.

BASIC PARAMETERS FOR RPA

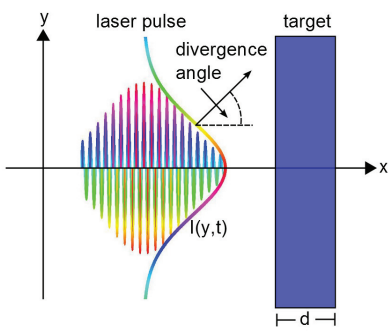

Figure 1: Typical setup for laser acceleration: A laser pulse enters the domain from the left and hits a target of thickness d.

A typical setup for laser ion acceleration is shown in Fig. 1. The target of thickness d consists of ions and electrons with thermal distribution. A laser pulse enters the domain from the left boundary. For a first insight to the radiation pressure acceleration, one can treat the target foil as a solid body with immutable shape. Taking into account the relativistic Doppler shifting, the equation of motion for the foil is given by:

$$\frac{d}{ds}\frac{\beta}{\sqrt{1-\beta^2}} = \sqrt{\frac{1-\beta}{1+\beta}}\frac{(1+R)I_0\tau}{\rho d c^2} f(s). \qquad (1)$$

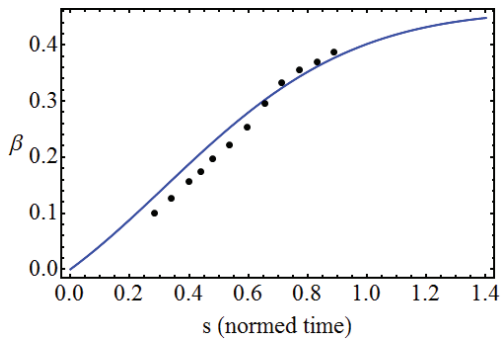

Figure 2: Comparison of β from Eq. 1 (blue line) and 1D PIC simulation (black dots), as a function of time s.

Where $s = t/\tau$ a dimensionless time, $\beta = v/c$, ρ target density, d target thickness, R reflection index, τ the overall laser period, I_0 maximum intensity of the laser and $f(s)$ the time-shape of the laser intensity. Usually $f(s)$ is given by a Gaussian function of FWHM τ eclipsed with an oscillation of frequency ω. The reflection index R is given by $R = (1-N/1+N)^2$, with $N = \sqrt{\epsilon_r}$[1] being the rarefractive index of the foil. For a plasma this holds:

$$N = \sqrt{\epsilon_r} = \sqrt{1 - \frac{\omega_p^2}{\omega^2}}\,. \qquad (2)$$

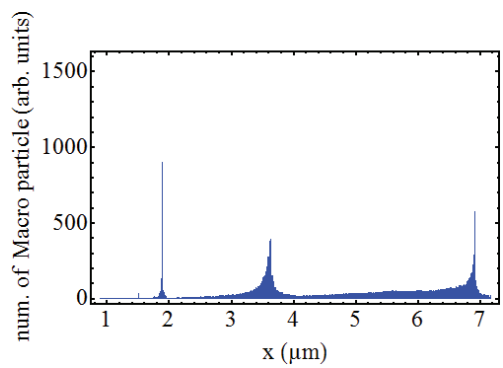

Figure 3: Spatial peak spectra from the 1D PIC simulation for different times. The peak has an energy of ≈ 3.82 GeV and density $n \approx 10^{29}$ m^{-3}. Similar behavior as in Fig 5.

Where ω is the laser frequency and $\omega_p^2 = n_e e^2/\epsilon_0 m_e$ is the plasma frequency of the electrons. For a metal foil target,

* Work supported by HIC for FAIR and HGS HIRe
† p.schmidt@gsi.de
‡ o.boine-frankenheim@gsi.de
§ i.hofmann@gsi.de

[1] For complex N one has to take the absolute value.

ISBN: 978-3-95450-132-8 doi:10.18429/JACoW-IPAC2014-TUPME031

usually $n >> n_c$ holds, so that R can be assumed as one: $R \approx 1$. For comparison, a 1D PIC simulation is performed with the software VSim© [8]. The target is a $d = 25$ nm thick titanium film with a particle density $n \approx 1000 n_c$. A circular polarized laser with an intensity of $I_0 = 5 \cdot 10^{21}$ Wcm^{-2} and a pulse length of $\tau = 65$ fs is used (see Fig. 1). A comparison between Eq. 1 and the simulation is given in Fig. 2. Very well agreement is achieved, even for that simple model. Figure 3 shows the spatial distribution of the plasma for different times. The peak has a maximum kinetic energy of 3.82 GeV and $\beta = 0.39$.

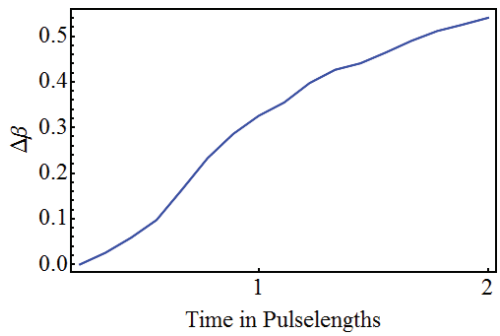

Figure 4: Evolution of the velocity spread $\Delta\beta = \beta_{max} - \beta_{min}$ as a function of time. After the laser is put off, $\Delta\beta$ increases further but saturates.

To ensure, that the accelerated plasma remains a sharp peak, the electron heating has to be suppressed. Therefore one uses a circular polarized laser. Moreover, the skin-depth of the laser $\delta = c/\omega_p$ has to be much smaller than the foil thickness d. If the electrical field strength of the laser E_l is much smaller than the coulomb attraction within the Debye-sphere $E_l << E_C$, the plasma stays quasi-neutral. This leads to a condition for the Debye-length λ_D:

$$\lambda_D^2 << \frac{e}{4\pi\epsilon_0 E_l}. \tag{3}$$

Since $\lambda_D^2 = \epsilon_0 k_B T_e / n_e e^2$ from Eq. 3 one can gain a critical electron temperature T_c. Electrons that are heated up above this temperature $T_e >> T_c$, are pushed away by the laser pulse. From Fig. 4 one obtains that, the velocity spread of the accelerated plasma increases over time and finally saturates. Therefore the simple model from Eq. 1 is not satisfactory.

MHD ONE-FLUID MODEL

To get a deeper insight of the process, a 1D fluid simulation is setup with the PDE solver package FiPy [9] using the Finite Volume Method (FVM). The plasma is modeled as a neutral gas of infinite conductivity with an isentropic equation of state. The system of normalized (non-relativistic) coupled PDEs then reads:

$$\frac{\partial n}{\partial \tau} + \nabla_\xi (n\vec{\beta}) = 0, \tag{4}$$

$$\frac{\partial \vec{\beta}}{\partial \tau} + (\vec{\beta}\nabla_\xi)\vec{\beta} = -k^2 n^{\varkappa - 1}\nabla_\xi n + \frac{a_0^2}{n}(\nabla_\xi \times \vec{B}) \times \vec{B}, \tag{5}$$

$$\frac{\partial \vec{B}}{\partial \tau} = \nabla_\xi \times (\vec{\beta} \times \vec{B}). \tag{6}$$

Where $\vec{\xi} = \vec{x}/L$ is a normed length and $\tau = t/T$ a normed time with the correlation $L = cT$. The parameter $k^2 = \varkappa k_B T_e / mc^2$ denotes the ratio between thermal- and rest energy of a fluid particle, $a_0^2 = 2I_0/\rho_0 c^3$ the ratio of laser energy density and rest energy of the fluid.

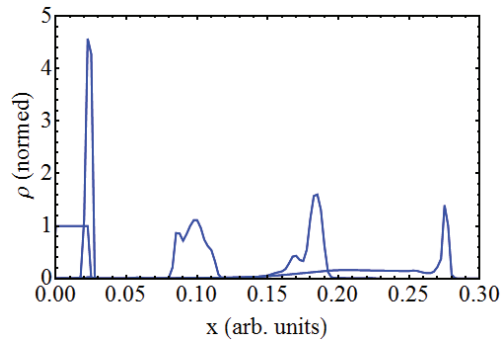

Figure 5: Spatial distribution of the plasma density, from the 1D fluid simulation, for different times. After a strong compression, the peak melts down.

As stated in section one, the electromagnetic wave of the laser has a finite penetration depth δ into the plasma. In the MHD model this is caused by Eq. 6: The induced current leads to a counteracting magnetic field, which displaces the original field. Figure 5 shows the spatial distribution of the plasma for different times: Due to a strong compression by the magnetic pressure $p_m = B^2/2\mu_0$ a shock wave is propagation into the plasma. After the acceleration stage, the field decay leads to a "melting" of the plasma in the penetration section. As shown in Fig. 3 this effect is also obtained in the 1D PIC simulation.

2D PIC SIMULATION

To analyse the transverse distribution (especially the divergence) of the RPA plasma, a 2D PIC simulation[2] (software VSim© [8]) is compared to a simplified fluid simulation (software FiPy [9]). For the RPA, the divergence is mainly determined by the opening angle of the laser pulse, since the acceleration points towards the propagation direction of the laser. The laser focus can be adequately modeled by a Gaussian. The intensity gradient from the center to the outer regions of the focus leads to a mass-flow. Both, the mass-flow and the opening angle of the laser pulse give the plasma its final shape (see Fig. 6). Figure 7 shows the result of the simplified fluid simulation, which solves the system of Eq. 4,5,6. The shape agrees very well with the one from

[2] In the present simulation, the parameters for target thickness, laser intensity and pulse length were scaled to save computational resources.

ISBN: 978-3-95450-132-8 doi:10.18429/JACoW-IPAC2014-TUPME031

the PIC simulation, especially the dense wings of the film can be observed.

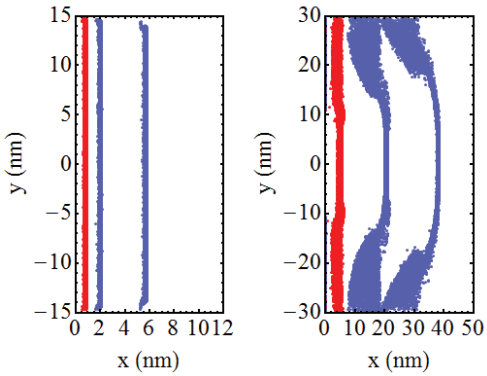

Figure 6: Particle distribution gained from a 2D PIC simulation a) in the case of a planar laser, b) for a gaussian laser profile.

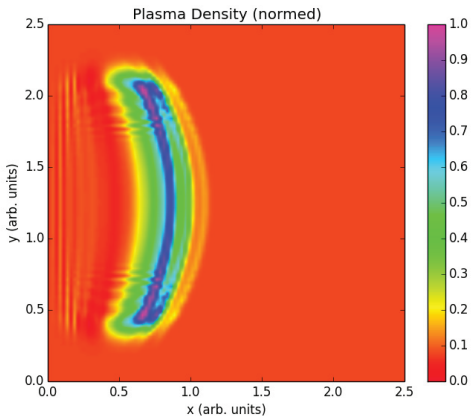

Figure 7: Density distribution from the 2D fluid simulation. A strong shock wave is observed with a mass transport from the center towards the outer regions (compare Fig 6). Furthermore the simulation shows a delution fan behind the shock wave.

To investigate on the neutrality degree of the plasma, one has to consider Fig. 8. Figure 8 shows the charge-density ρ_e contour plot in the xy-plane. The electrons form a sharp front (blue) followed by the ions (red). This indicates, that the acceleration mechanism proceeds the following way: A compression wave of electrons runs into the target and forms a sharp front which drags the ions by its electrical field. Since the electrical field is much stronger (due to much higher particle number) than in the TNSA case, this acceleration mechanism produces a sharp peak.

CONCLUSIONS AND OUTLOOK

Basic requirements for a radiation pressure acceleration in terms of simple parameters and equations are obtained by a 1D model. This leads to some fundamental constrains for the electron density n_e and temperature T_e. For a given laser

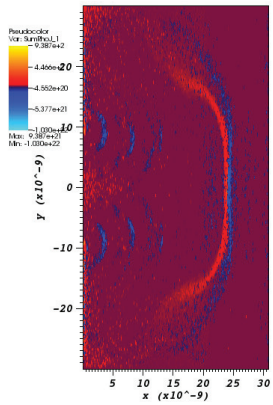

Figure 8: Charge distribution ρ_e from the 2D PIC simulation. A strong negative charge (blue) from an electron front is followed by a sharp positive charge (red) caused by the ions. the wine-red regions are neutral. Furthermore a delution fan is observed as in the fluid case (Fig. 7).

intensity the critical electron temperature T_c can be derived from Eq. 3. Good agreement between PIC simulation and fluid simulation was achieved in 1D and 2D. From that, the underlying mechanism can be stated. From a 2D simulation the transversal distribution of the plasma is gained. Since the laser has a Gaussian shape and transversal opening angle, the plasma shows large divergence, too. Further investigation will be laid on a more precise description of the longitudinal and transversal divergence. Therefore a two-fluid model (electron- and ion gas) will be developed.

REFERENCES

[1] S. Busold et. al., Proc. of PAC 2011 Conference, p. 1960, New York, USA (2011).

[2] V. Bagnoud et al., App. Phys. B 100, 137-150 (2010).

[3] S. C. Wilks et al., "Energetic proton generation in ultra-intense laser-solid interactions", Phys. Plasmas, Vol 8 No 2 (2001).

[4] M. Passoni et al., "Target normal sheath acceleration: theory, comparison with experiments and future perspectives", New Journal of Physics Vol 12, 045012 (14pp) (2010).

[5] P. Mora et al., "Rarefaction shock in plasma with a bi-Maxwellian electron distribution function", Phys. Rev. E Stat. Nonlin. Soft Matter Phys., Vol 84, 036402 (2011).

[6] S. Kar et al., "Ion Acceleration in Multispecies Targets Driven by Intense Laser Radiation Pressure", Phys. Rev. Lett. (109), 185006 (2012).

[7] A. Henig et al., Phys. Rev. Lett. (103), 245003 (2009).

[8] Tech-X Corporation: VSim©, URL: www.txcorp.com, Boulder, USA (2012).

[9] J. E. Guyer, D. Wheeler, J. A. Warren, Computing in Science and Engineering 11(3) pp. 6-15 (2009).